Si - Bi$_2$Te$_3$ PHOTOCONVERTER DETECTORS

G.M. AHMADOV[a], G.B. IBRAGIMOV[a,b], M.A. JAFAROV[b]

[a]Institute of Physics, Ministry of Science and Education of the Republic of Azerbaijan
AZ 1143, G. Javid Avenue 131, Baku, Azerbaijan
[b]Baku State University, Baku, Azerbaijan, Maarif.Jafarov@mail.ru

Bismuth telluride (Bi$_2$Te$_3$) photoconverter detector based on Si single crystal is presented. The photo-reactions of the obtained photodetectors in infrared radiation with wavelengths of 1064 nm and 1550 nm were studied at room temperature. Linear dependences of the photocurrent on both the power of the incident light and the applied voltage were observed. Key device parameters, including photosensitivity and quantum efficiency, were calculated.

INTRODUCTION

The integrated circuit (IC) industry has rapidly developed following Moore's Law for over half a century. However, Moore's law is reaching its end when the transistors are finally scaled down to several nanometers, and the quantum effects and heat dissipation problems have become dominant [1-3]. Silicon (Si) photonics have emerged as one of a few potential technologies to extend the lifetime of Moore's Law, or, in other words, to open the "post Moore era" [4,5]. Si photonics can provide high transmission speed, high bandwidth, low power consumption, low heat dissipation, etc., utilizing the advantages of light over electrons. In recent years, many significant breakthroughs of Si based passive and active building blocks on and in Si have been demonstrated including waveguides, electro-optic modulators, ultrafast photodetectors, fiber-to-waveguide couplers, and lasers [7]. Among all the elementary components, a high performance near infrared photodetector is crucial to make a high speed optical link for either optical telecommunications or interconnects [8]. Conventionally, there are two kinds of absorbent materials at the telecom wavelength utilized for photon detection on Si: germanium (Ge)-on-Si[5] and III-V-on-Si [9]. Here, we have put forward a topological insulator (TI) based photodetector on Si, which is compatible with complementary metal-oxide-semiconductor (CMOS) technology and can be monolithically integrated on Si.

Bismuth telluride (Bi$_2$Te$_3$) together with Bi$_2$Se$_3$ and Sb$_2$Te$_3$ was theoretically predicted and experimentally proved to be a typical 3-dimensional (3D) TI with a single Dirac cone on the surface. Molecular beam epitaxy (MBE), chemical vapor deposition [10], and pulsed laser deposition techniques [11] have been adopted in the fabrication of high-quality TI films of Bi$_2$Se$_3$, Bi$_2$Te$_3$, and Sb$_2$Te$_3$ on substrates including sapphire [12], SrTiO$_3$[13], and also Si.

Many theoretical studies have been focused on the response of the surface states to light, and several worthy progressive studies have been reported, including the Dirac surface state assisted high-performance broadband photodetection from infrared to terahertz [14], the circularly polarized light induced helicity-dependent current [15], the nonlinearity induced passive mode-locked lasers [16], the warping effect enhanced relative signal-to-noise ratio (SNR) [17], and the linearly polarized light induced polarization dependent photocurrents[18].

Zhang et al [19]. predicted that the surface state can have strong optical absorption. The surface absorption is determined by the fine-structure constant *a*, and it is uniform and independent of the wavelength.

In this letter, Si-based Bi$_2$Te$_3$ photodetectors with responses to 1064 nm and 1550 nm light illumination at room temperature are demonstrated. This study shows that TI based photodetectors could be one of the candidate detectors for future Si photonics.

EXPERIMENT

The following conditions were used to prepare the electrolyte solution used. According to the Pourbaix diagrams, in pH=0 solutions, Bi and Te exist as completely dissolved Bi^{3+} and HTeO$_2^+$, respectively. The electrolyte was prepared with water (18 MΩcm resistivity) collected from Barnstead E-pure filtration system. First Bi(NO$_3$)$_3$.5H$_2$O (purity 99% analytical grade, Aldrich-Sigma) and TeO$_2$ (purity 99%) were dissolved in 1M HNO$_3$. The two solutions were then mixed and the mixture was adjusted to pH=6. All electrochemical depositions were done at room temperature using conventional three–electrode system and a potentiostat (Gamry Reference 600). PTFE reaction cell was used where the working electrode was placed horizontally at the bottom. Gold coated silicon wafer and Platinum mesh were used as working and counter electrodes, respectively. Ag/AgCl with 3M KCl electrolyte was used as the reference electrode. Bi$_2$Te$_3$ thin films were prepared by the continuous electrodeposition method of which a constant voltage was applied. The gold working electrode was made as a gold-coated silicon wafer (n-Si (111) with a resistivity < 0.02 Ω cm). This coating of gold on the silicon wafer was done by first cleaning the silicon wafer by ultra sonication in organic solvents. Then it was exposed to

a mild oxygen plasma treatment (PE/RIH, 50 W) for 2 min to remove the organic contamination and surface particles. Before this wafer was placed in the reaction cell, an In-Ga eutectic was coated on the unpolished backside of the silicon wafer as an ohmic contact.

Then, the Ti electrodes were achieved by electron beam evaporation on top of the Bi$_2$Te$_3$ film, which exhibits a linear dependence, suggesting that ideal Ohmic contacts were formed between the electrodes and the Bi$_2$Te$_3$ film from the I–V test in the dark.

RESULT AND DISCUTION

The incident power range for 1064 nm and 1550 nm was 0.67–2.8 mW and 0.194–0.389 mW, respectively. All the measurements were carried out at room temperature. The responsivity (R) and quantum efficiency (η) of this device were calculated according to the following equations, respectively [20]:

$$R = \frac{I_{ph}}{P_{opt}}$$
(1)

$$\eta = R\left(\frac{hc}{q\lambda}\right)$$
(2)

where I_{ph}, P_{opt}, h, c, q and k are the photocurrent, the light power of the effective illuminated area, the Planck's constant, the light velocity in vacuum, the electron charge, and the wavelength of incident light, respectively.

Figure 1 presents the AFM image of the Bi$_2$Te$_3$ film. The root mean square (RMS) roughness of the Bi$_2$Te$_3$ film is 1.29 nm. Surface steps with a height of 1 nm can be observed clearly, which correspond to the thickness of a quintuple layer with five Te-Bi-Te-Bi-Te atomic layers. The existence of clear surface steps indicates high crystal quality.

Photocurrent under different bias voltages and light powers was investigated, and the results after the removal of the background current are shown in Figure 2. Figures 2(a) and 2(c) present the photocurrent of a typical device under different incident powers at the wavelength of 1064 nm and 1550 nm, respectively. Obviously, the photocurrent exhibits a high dependence on the bias voltage and the incident light power. Along with the increasing bias voltage, an approximately linear increasing tendency of photocurrent can be observed. Given the fact that the bias voltage facilitates the separation and transport of photon-excited carriers, collection of photo- generated carriers will increase significantly with the increase in the electric field.

It is obvious that at the higher excitation intensity, more electron-hole pairs are generated, which is consistent with the observed fact that the photocurrent increases monotonously with the increase in the excitation power. In order to have a more intuitive observation of the photocurrent-excitation power relation, the photocurrent under different excitation powers at 0.1 V is plotted and linearly fitted in Figures 3(b) and 3(d) for 1064 nm and 1550 nm, respectively.

Based on Eq. (1), Eq. (2), and the slope of the linear fitting curve, the responsivity for the device is 3.64 x 10^{-3} AW^{-1} for 1064 nm and 3.32 x 10^{-2} AW^{-1} for 1550 nm, respectively. The quantum efficiency is 0.424% for 1064 nm and 2.66% for 1550 nm.

The relationship of the incident light intensity-absorption coefficient for Bi$_2$Te$_3$ follows Eq. (3), where I, I$_O$, a, and d represent the light intensity, original incident light intensity, absorption coefficient, and thickness of the Bi$_2$Te$_3$ film, respectively. There are two interfaces of the device, Bi$_2$Te$_3$ and Si and Bi$_2$Te$_3$ and air. Reflections exist for both the interfaces. The interfacial reflection coefficients between air and Bi$_2$Te$_3$ are up to 53% for 1064 nm and 60% for 1550 nm, while those between Bi$_2$Te$_3$ and Si are 7.8% for 1064 nm and 14.7% for 1550 nm.[24] The absorption coefficients for different incident light wavelengths are also distinct, which are 7.0 x 10^5 cm^{-1} for 1064 nm and 4.2 x 10^5 cm^{-1} for 1550 nm, respectively.
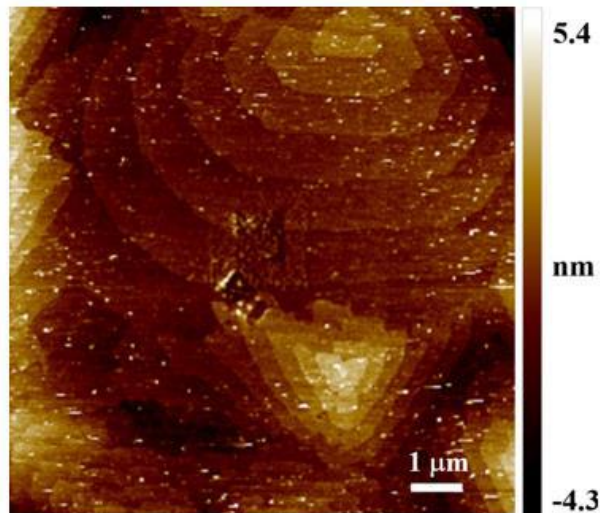

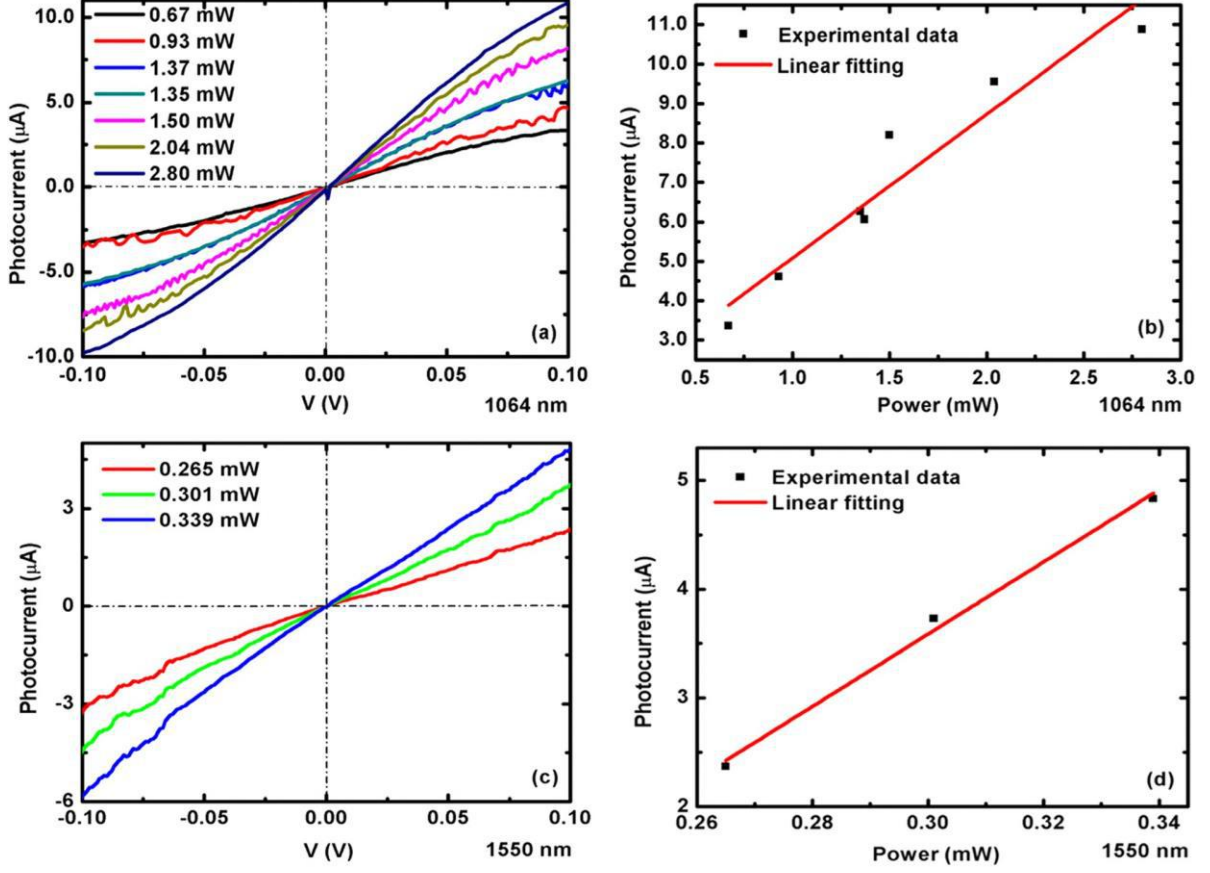*Fig. 1.* AFM image of the Bi$_2$Te$_3$ film on Si.

Fig. 2. Typical photocurrent-voltage curves of the Bi$_2$Te$_3$ photodetector at different incident powers under 1064 nm (a) and 1550 nm (c) illumination, respectively. (b) and (d) show the photocurrent under different excitation powers at 0.1 V corresponding to (a) and (c), respectively. The red line is a linear fit of the data points.

After multiple reflections, the relationship of the light intensity after absorption by the Bi$_2$Te$_3$ film and the original incident light intensity can be expressed by Eq. (4), where I_1, R_C, and R_C' represent the light intensity after absorption by the Bi$_2$Te$_3$ film, reflection coefficient between air and the Bi$_2$Te$_3$ film, and reflection coefficient between the Bi$_2$Te$_3$ film and Si, respectively.

$$I = I_O e^{-ad} \tag{3}$$

$$I_\infty = \frac{R_C + (1 - R_C)(1 - R'_C)e^{-ad}}{1 - (1 - R_C)R'_C e^{-2ad}} I_O \tag{4}$$

Obviously, the reflection of most of the incident light has been caused by the large reflection rate. Considering this non-negligible loss, the quantum efficiency can be revised by dividing 0.457 for 1064 nm and 0.358 for 1550 nm (the other portion is reflected by the interfaces and transmitted into Si). After revision, the internal quantum efficiency of the device is 0.9% under the wavelength of 1064 nm, and it corresponds to 7.4% for the case of 1550 nm. Under the same incident power, the longer wavelength leads to a larger number of photons, thereby a higher photocurrent and larger responsivity are expected. The performance of the present device in terms of responsivity and quantum efficiency is much better

than those of the published polycrystalline Bi$_2$Te$_3$ based devices. The responsivity is 2–3 orders higher.

For Bi$_2$Te$_3$, the bandgap measured by angle-resolved photoemission spectroscopy is 0.165 eV while that for Si is 1.12 eV. The photocurrent would mainly consist of four parts: the photoconductivity effect of the Bi$_2$Te$_3$ bulk and the surface states, transitions between the surface states and the bulk states, and the contribution of Si. For illumination at 1064 nm, Si shows little absorption to the incident light since most light is absorbed by Bi$_2$Te$_3$ before reaching Si.

CONCLUSION

In summary, we reported a monocrystalline Bi$_2$Te$_3$ photoconductive detector on Si grown by electrochemical technology and can be monolithically integrated on Si. The as-fabricated photodetector exhibits a high response to photons at 1064 nm and 1550 nm at room temperature. The responsivity and the quantum efficiency are much better than polycrystalline Bi$_2$Te$_3$ based devices. The responsivity and the internal quantum efficiency of the device are 3.64 x 10^{-3} AW^{-1} and 0.9% for 1064 nm and 3.32 x 10^{-2} AW^{-1} and 7.4% for 1550 nm, respectively. This study suggests that the Bi$_2$Te$_3$ photodetectors have potential applications in future Si photonics.

[1] *M.M. Waldrop.* Nat.News 530, 144, 2016.

[2] *D. Liang and J.E. Bowers.* Nat.Photonics4, 511, 2010.

[3] *R. Soref.* IEEEJ. Sel. Top. Quantum Electron. 12, 1678, 2006.

[4] *Bothpho Osmond, D. Marris-Morini, P. Crozat, E. Cassan, J. M.F'ed'eli, S. Brision, J. F. Damlencourt, V. Mazzochi, D. Van Thourhout and J. Brouckaert.* in IEEE International Conference on Group IVPhotonics GFP. 2009, Vol. 1, p. 10.

[5] *L. Chen, P. Dong and M. Lipson.* V Opt. Express 16,11513, 2008.

[6] *S. Feng, Y. Geng, K. M. Lau, and A. W. Poon.* IEEE InternationalConference on Group IV Photonics GFP 2012, Vol. 37, p. 51.

[7] *Y.L. Chen, J.G. Analytis, J.H. Chu, Z.K. Liu, S.K. Mo, X.L. Qi, H.J. Zhang, D.H. Lu, X. Dai, Z. Fang, S. C. Zhang, I.R. Fisher, Z. Hussain, and Z.X. Shen.* Science 325, 178, 2009.

[8] *H. Zhang, C. Liu, X. Qi, X. Dai, Z. Fang, and S. Zhang.* Nat. Phys. 5,438, 2009.

[9] *Y.Y. Li, G. Wang, X.G. Zhu, M.H. Liu, C. Ye, X. Chen, Y.Y. Wang, K. He, L.L. Wang, X.C. Ma, H.J. Zhang, X. Dai, Z. Fang, X.C. Xie, Y. Liu, X.L. Qi, J.F. Jia, S.C. Zhang, and Q.K. Xue.* Adv.

Mater. 22, 4002, 2010.

[10] *H. Cao, R. Venkatasubramanian, C. Liu, J. Pierce, H. Yang, M.Z. Hasan, Y. Wu, and Y.P. Chen.* Appl. Phys. Lett. 101,162104, 2012.

[11] *H. Zhang, J. Yao, J. Shao, H. Lu, S. Li, D. Bao, C. Wang, and G. Yang.* Sci. Rep. 4, 5876 (2014).

[12] *K. Zheng, L.B. Luo, T.F. Zhang, Y.H. Liu, Y.Q. Yu, R. Lu, H.L. Qiu, Z.J. Li, and J.C. Andrew Huang,* J.Mater. Chem. C3, 9154, 2015.

[13] *P.H. Le, K.H. Wu, C.W. Luo, and J. Leu.* Thin Solid Films 534,659, 2013.

[14] *X. Zhang, J. Wang, and S.C. Zhang.* Phys. Rev. B 82, 245107, 2010.

[15] *P. Hosur.* Phys. Rev.B83,035309 (2011).

[16] *J. Koo, J. Lee, C. Chi, and J.H. Lee.* J.Opt.Soc.Am.B31, 2157 (2014).

[17] *J. M. Shao, H. Li, and G.W. Yang.* Nanoscale6,3513, 2014.

[18] *J.D. Yao, J.M. Shao, S.W. Li, D.H. Bao, and G.W. Yang.* Sci.Rep.5,14184, 2015.

[19] *F. Xia,T. Mueller,Y. Lin, A. Valdes-Garcia, and P. Avouris.* Nat.Nanotechnol. 4, 839, 2009.

[20] *X. Gan, R. J. Shiue, Y. Gao, I. Meric, T. F. Heinz, K. Shepard, J. Hone, S.Assefa, and D. Englund.* Nat. Photonics 7, 883, 2013.